

## Rapid Synthesis of High-Entropy Metal Sulfides under Ambient Conditions as Efficient Catalysts for Urea Oxidation Reaction

Linwei Jiang,<sup>a</sup> Yee Xuan Seow,<sup>a</sup> Hsien-Yi Hsu,<sup>b</sup> Mark A. Buntine,<sup>a</sup> Hongpeng Jia,<sup>\*c</sup>

Zongyou Yin,<sup>\*d</sup> and Guohua Jia<sup>\*a</sup>

<sup>a</sup> School of Molecular and Life Sciences, Curtin University, Perth, WA 6102, Australia

<sup>b</sup> School of Energy and Environment, Department of Materials Science and Engineering,  
Centre for Functional Photonics (CFP), City University of Hong Kong, Hong Kong, China

<sup>c</sup> CAS Center for Excellence in Regional Atmospheric Environment, and Key Laboratory  
of Urban Pollutant Conversion, Institute of Urban Environment, Chinese Academy of  
Sciences, Xiamen 361021, China. Email: [hpjia@iue.ac.cn](mailto:hpjia@iue.ac.cn)

<sup>d</sup> Research School of Chemistry, The Australian National University, Canberra, ACT 2601,  
Australia. Email: [zongyou.yin@anu.edu.au](mailto:zongyou.yin@anu.edu.au)

*\* Corresponding author.*

*Email:* [guohua.jia@curtin.edu.au](mailto:guohua.jia@curtin.edu.au); [hpjia@iue.ac.cn](mailto:hpjia@iue.ac.cn), [zongyou.yin@anu.edu.au](mailto:zongyou.yin@anu.edu.au)

## 1. Experimental

### 1.1. Materials

Sodium sulfide hydrate ( $\text{Na}_2\text{S}\cdot\text{xH}_2\text{O}$ ,  $\geq 60\%$ ), ruthenium(III) chloride trihydrate ( $\text{RuCl}_3\cdot 3\text{H}_2\text{O}$ ), manganese (II) chloride tetrahydrate ( $\text{MnCl}_2\cdot 4\text{H}_2\text{O}$ ), cobalt (II) chloride hexahydrate ( $\text{CoCl}_2\cdot 6\text{H}_2\text{O}$ ), nickel(II) chloride hexahydrate ( $\text{NiCl}_2\cdot 6\text{H}_2\text{O}$ ), iron(II) chloride tetrahydrate ( $\text{FeCl}_2\cdot 4\text{H}_2\text{O}$ ), urea and potassium hydroxide (KOH, 90%) were acquired from Sigma Aldrich. Nafion solution (5 wt.% in lower aliphatic alcohols and water) were procured from Fuel Cell Store. Commercial Pt/C catalyst containing 20 wt% platinum supported on carbon (Pt/C, 20 wt%), purchased from Suzhou Shnerio Technology supplier. All chemical reagents were directly used as supplied, without undergoing any further treatment. All aqueous solutions were prepared with ultrapure water ( $18.2\text{ M}\Omega$ ).

### 2.2 Synthesis method of NiS, (NiCoRu)S and HES nanoparticles

A mixed-metal precursor solution was prepared by dissolving 0.1 mmol of  $\text{MnCl}_2\cdot 4\text{H}_2\text{O}$ ,  $\text{CoCl}_2\cdot 6\text{H}_2\text{O}$ ,  $\text{NiCl}_2\cdot 6\text{H}_2\text{O}$ ,  $\text{RuCl}_3\cdot 3\text{H}_2\text{O}$  and  $\text{FeCl}_2\cdot 4\text{H}_2\text{O}$  in 25 mL ultrapure water, yielding a dark brown solution. In parallel,  $\text{Na}_2\text{S}\cdot\text{xH}_2\text{O}$  (100 mg) was dissolved in 5 mL ultrapure water to generate the sulfide source. The metal chloride solution (5 mL) was then rapidly injected into the sulfide solution under vigorous stirring at room temperature. The precipitate was separated by centrifugation (7000 rpm, 5 min), redispersed in ethanol with sonication, and washed twice to remove residual impurities. The resulting high-entropy sulfide nanoparticles were dried under vacuum at  $60\text{ }^\circ\text{C}$  overnight. For the synthesis of comparison samples such as NiS and ternary (NiCoRu)S, the same procedure was employed by dissolving the corresponding metal chlorides (0.1 mmol for each constituent)

in 5 mL ultrapure water, followed by rapid injection into the  $\text{Na}_2\text{S}$  solution under identical conditions. The products were collected and purified in the same method as described above.

### 2.3 Materials Characterization

X-ray diffraction (XRD) measurements were performed on a Panalytical Empyrean X'pert PRO diffractometer operated at 40 kV and 40 mA, using  $\text{Cu K}\alpha$  radiation ( $\lambda = 1.54 \text{ \AA}$ ). X-ray photoelectron spectroscopy analysis was carried out on a Kratos Axis Ultra system equipped with a monochromatic  $\text{Al K}\alpha$  source (1486.6 eV, 10 kV, 10 mA) and a hybrid lens. For transmission electron microscopy (TEM), a dilute suspension of high-entropy sulfide particles was drop-cast onto carbon-coated copper grids, producing a thin and uniform particle layer that reduced aggregation and facilitated high-resolution imaging of morphology and structure. High-angle annular dark-field scanning transmission electron microscopy (HAADF-STEM), electron energy-loss spectroscopy (EELS) and energy-dispersive X-ray spectroscopy (EDS) mapping were conducted on a FEI Titan G2 80–200 KV microscope at the Centre for Microscopy, Characterization and Analysis (CMCA), University of Western Australia. AFM measurements were conducted using a Bruker Dimension Icon atomic force microscope equipped with a Bruker NCHVA probe. Elemental concentrations were quantified at ChemCentre, Western Australia. Specifically, the concentration of Fe was determined via Inductively Coupled Plasma Optical Emission Spectrometry (ICP-OES), while Ni, Co, Mn, and Ru were analyzed using Inductively Coupled Plasma Mass Spectrometry (ICP-MS).

### 2.4 Electrochemical measurements

The electrochemical investigations were performed utilizing a CS2350M (WUHAN CORTEST INSTRUMENTS CORP., LTD.) electrochemical analyzer configured in a conventional three-electrode configuration. The electrochemical cell incorporated a graphite rod auxiliary electrode and a Hg/HgO reference system. The experimental protocols were executed under ambient conditions, with all measured potentials being standardized against the reversible hydrogen electrode (RHE) scale through the following potential conversion relationship:  $E_{\text{RHE}} = E_{\text{Hg/HgO}} + 0.0591 \text{ pH} + 0.098 \text{ V}$ . To prepare the catalyst ink, 5 mg of catalyst powder was suspended in a mixture of 200  $\mu\text{L}$  deionized water, 280  $\mu\text{L}$  ethanol, and 20  $\mu\text{L}$  Nafion solution (5 wt%), followed by sonication for approximately 60 min to obtain a uniform dispersion. Subsequently, 50  $\mu\text{L}$  of the resulting ink was drop-cast onto a pre-cleaned nickel foam electrode ( $1 \times 1 \text{ cm}^2$ , loading  $\sim 50 \text{ } \mu\text{g cm}^{-2}$ ) and allowed to dry under ambient conditions. LSV measurements were conducted in an electrolyte of 1 M KOH and 0.5 M urea at a scan rate of  $5 \text{ mV s}^{-1}$  to evaluate the polarization behavior. To ensure measurement accuracy, all LSV data underwent ohmic compensation with a 95% iR correction factor applied to mitigate solution resistance effects. Electrochemical impedance spectroscopy (EIS) measurements were conducted within a frequency range of 0.05 Hz to 10 kHz, with an amplitude of 5 mV, under operational conditions. The electrochemical stability of urea oxidation was assessed using the i-t curve at a constant current of  $50 \text{ mA cm}^{-2}$ , without iR correction.

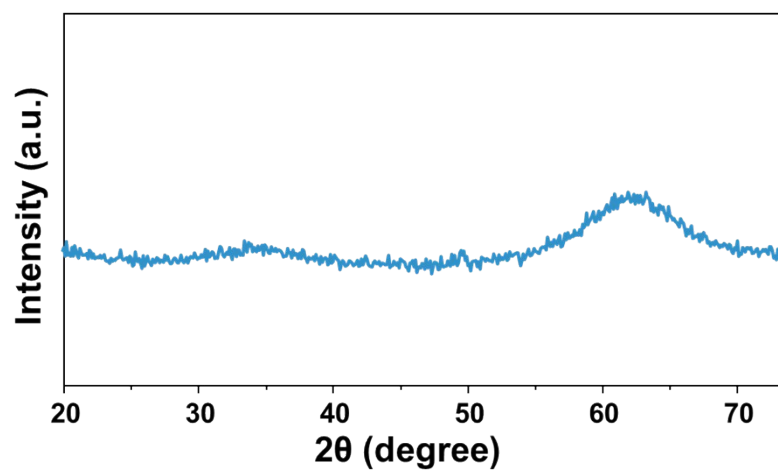


Figure S1. XRD pattern of NiCoFeMnRuS.

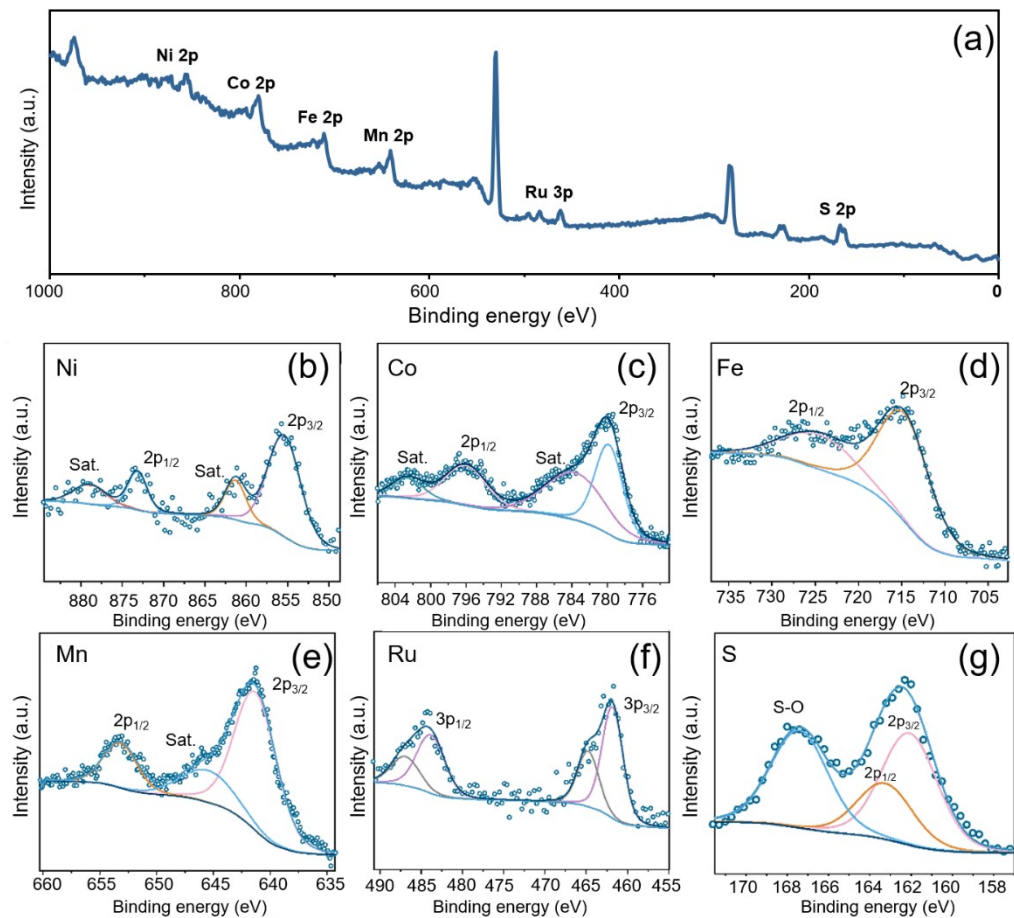


Figure S2. X-ray photoelectron spectroscopy (XPS) analysis of NiCoFeMnRuS high-entropy sulfide nanoparticles. (a) Full survey spectrum confirming the presence of Ni, Co, Fe, Mn, Ru, and S elements. High-resolution spectra of (b) Ni 2p, (c) Co 2p, (d) Fe 2p, (e) Mn 2p, (f) Ru 3p, and (g) S 2p regions.

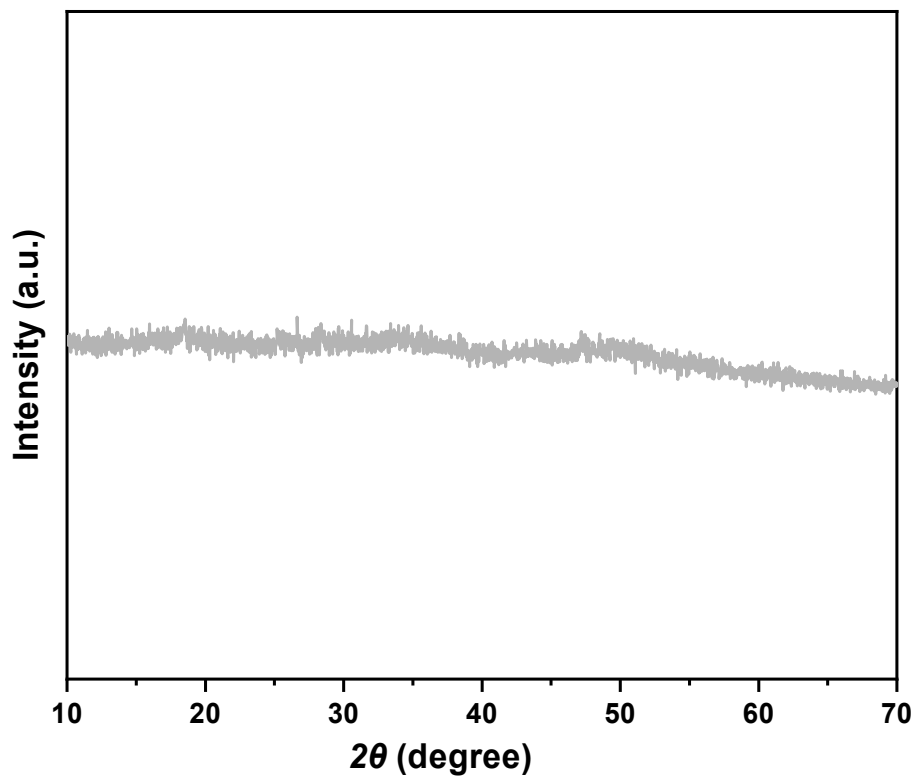


Figure S3. XRD pattern of NiCoRuS.

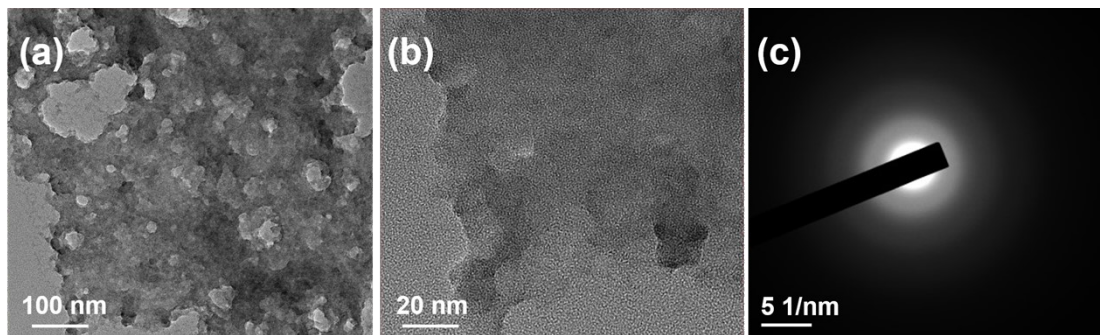


Figure S4. TEM images (a, b) and HRTEM images (c, d) of the NiCoRuS sample.

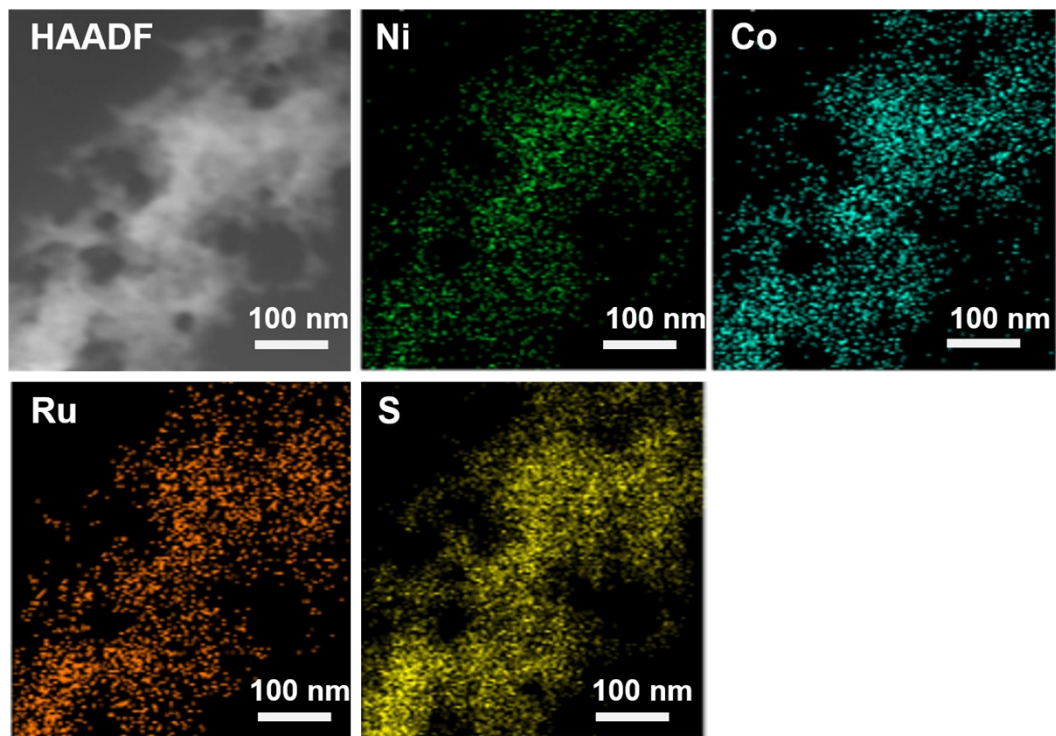


Figure S5. EDS mapping of NiCoRuS.

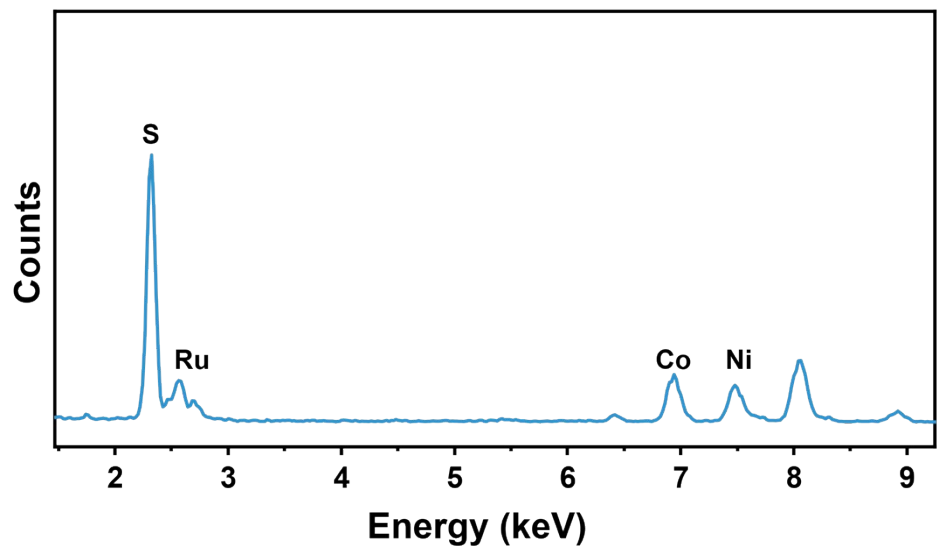


Figure S6. EDS spectra of NiCoRuS.

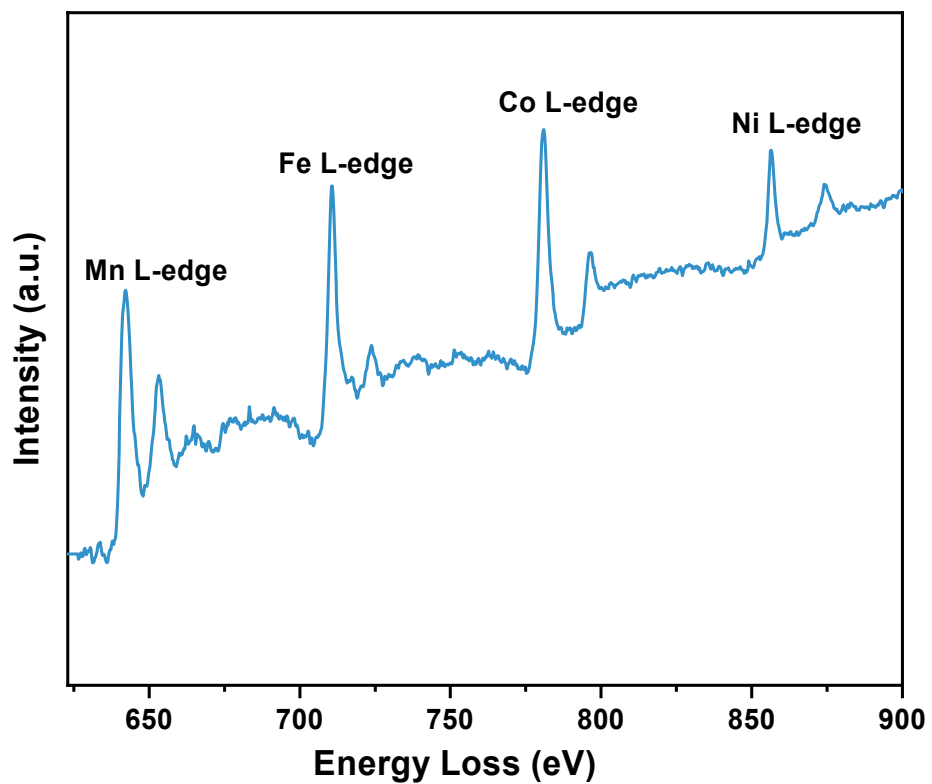


Figure S7. EELS spectrum showing Mn, Fe, Co, and Ni L-edges. The Ru M-edge is obscured by the C K-edge from the carbon support.

mple.

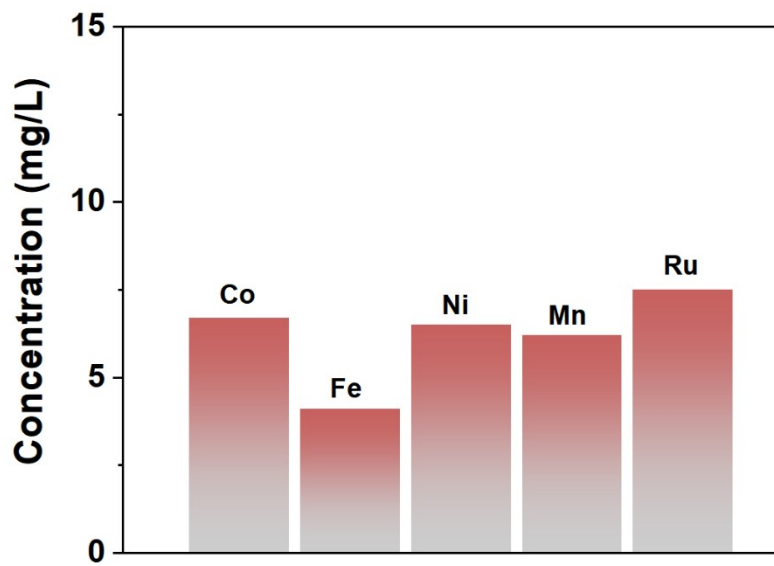


Figure S8. Elemental contents from the ICP-OES/MS test of NiCoFeMnRuS.

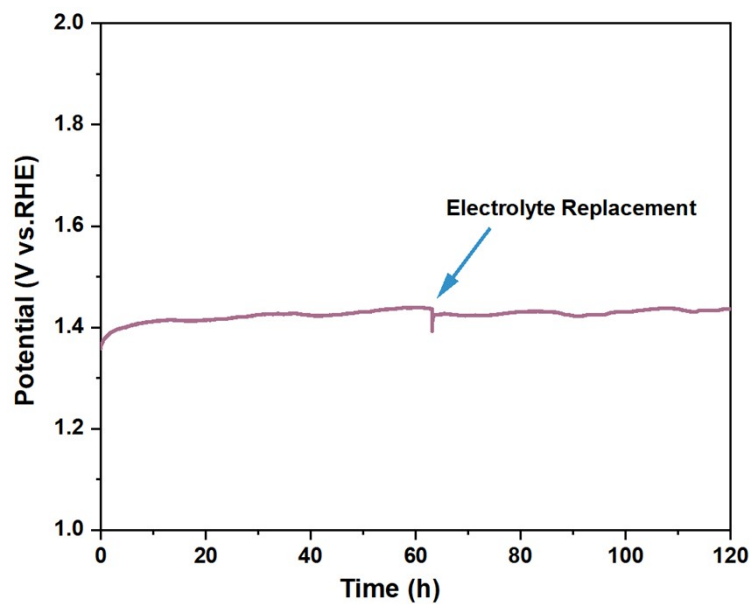


Figure S9. Chronoamperometric stability of NiCoFeMnRuS for 120 h in 1 M KOH + 0.5 M urea.

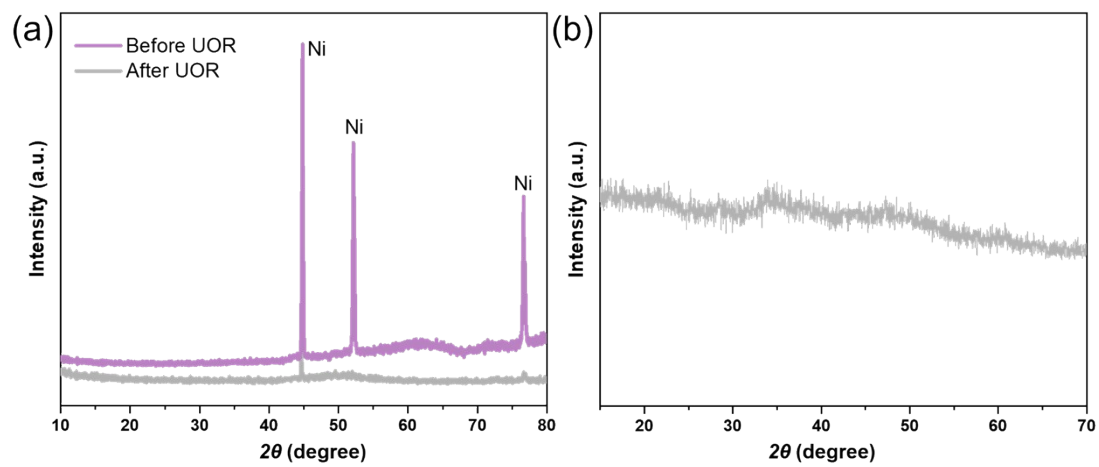


Figure S10. (a) XRD patterns of the NiCoFeMnRuS catalyst on nickel foam before and after UOR. (b) XRD patterns of NiCoFeMnRuS catalyst powder after UOR.

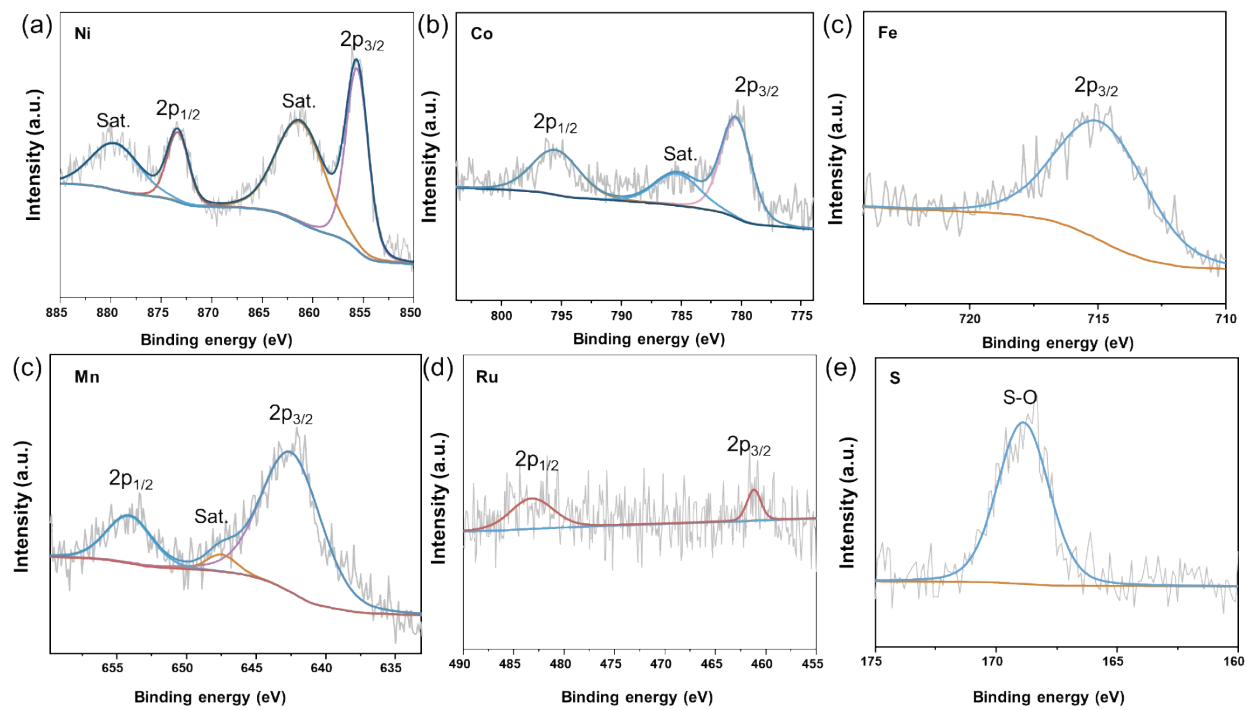


Figure S11. The XPS high-resolution spectra comparison of (a) Ni 2p, (b) Co 2p, (c) Fe 2p, (d) Mn 2p, (e) Ru 3p, (g) S 2p in NiCoFeMnRuS sample post UOR.

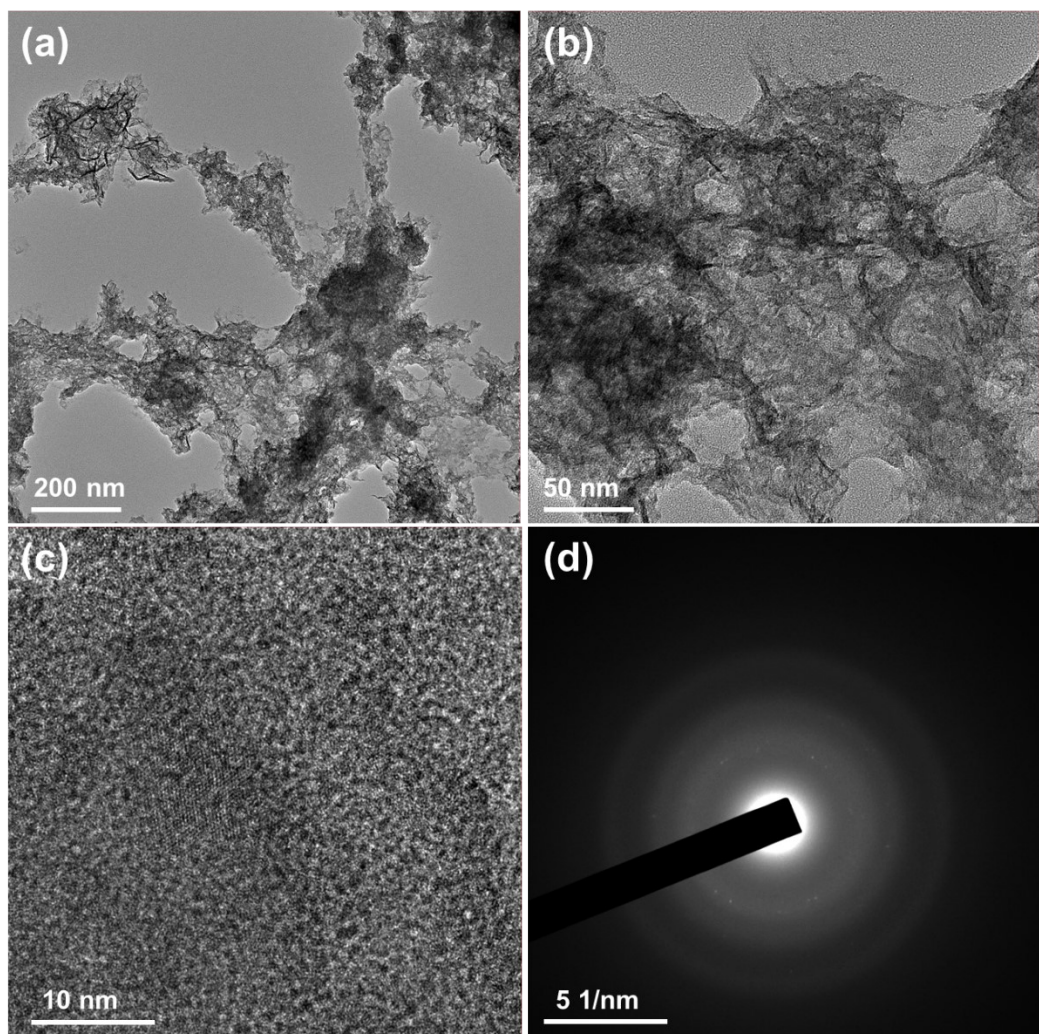


Figure S12. (a, b) TEM images, (c) HRTEM image, and (d) Selected area electron diffraction pattern of NiCoFeMnRuS after the UOR.

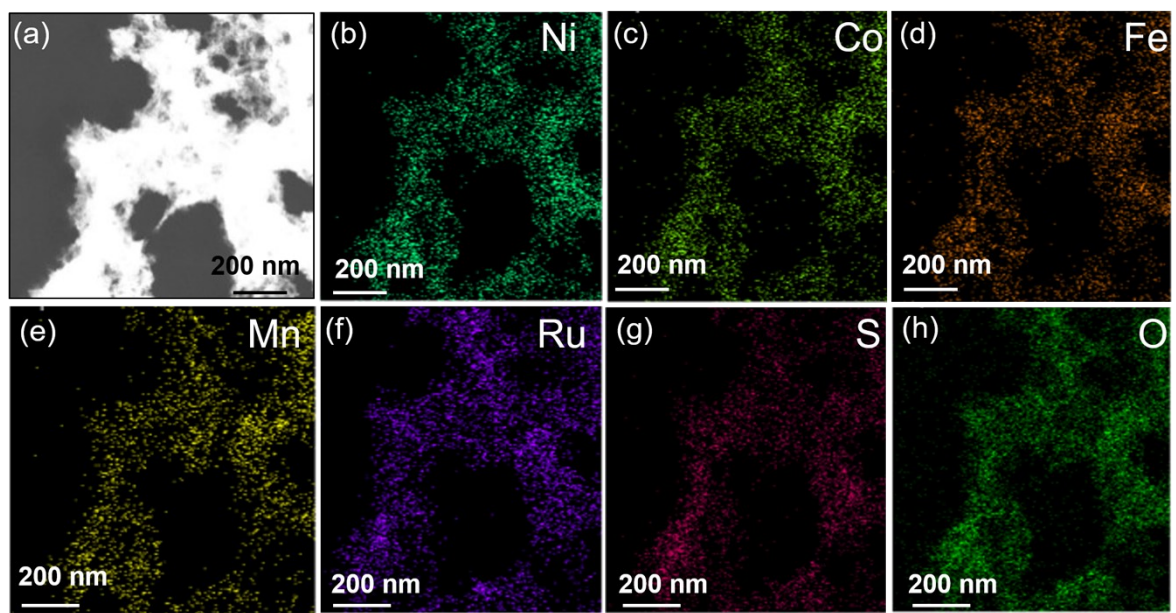


Figure S13. EDS mapping of NiCoFeMnRuS after UOR test.

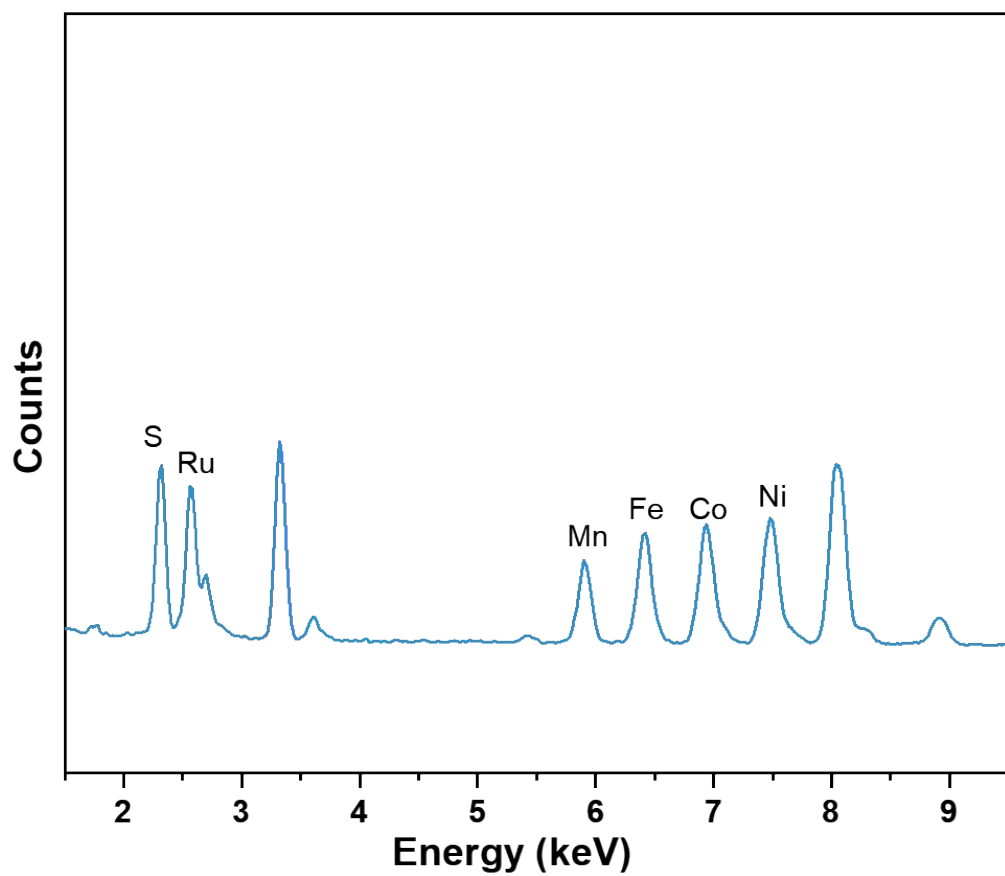


Figure S14. EDS spectra of NiCoFeMnRuS after UOR test.

**Table R1. Comparison of the reported catalysts for overall urea electrolysis in alkaline media**

Catalysts	Electrolyte	$\eta$ (mV)@ $j$ (mA cm $^{-2}$ )	References
FeNiS	1 M KOH + 0.5 M Urea	1.57@10	[1]
SnS/MnFe <sub>2</sub> O <sub>4</sub>	1 M KOH + 0.5 M Urea	1.52@10	[2]
NiCoS/CP	1 M KOH + 0.5 M Urea	1.6@10	[3]
CoS/NiS@CuS	1 M KOH + 0.5 M Urea	1.51@10	[4]
MoS <sub>2</sub> –MoO <sub>2</sub> /Ni <sub>3</sub> S <sub>2</sub>	1 M KOH + 0.5 M Urea	1.47 @ 10	[5]
NiS nanotubes	1 M KOH + 0.5 M Urea	1.445 @ 10	[6]
Ni–Fe–Co LDH@Ni–S	1 M KOH + 0.5 M Urea	1.42@ 10	[7]
Fe(OH) <sub>3</sub> /Ni <sub>3</sub> S <sub>2</sub> /NiS	1 M KOH + 0.33 M Urea	1.4@10	[8]
(NiCoFeMnRu)S    Pt/C	1 M KOH + 0.5 M Urea	1.382@10	This work

## Refence

- [1] T. Chen, Q. Guo, J. Ye, Q. Jiang, N. Chai, F.-Y. Yi, *ACS Appl. Nano Mater.* **2025**, *8*, 2730-2740.
- [2] P. Justin Jesuraj, G. John, M. Navaneethan, C. Min Lee, J. Mun, Y.-C. Kang, S. Yoon Ryu, *Inorg. Chem. Commun.* **2024**, *167*, 112686.
- [3] Y. Zeng, S. Lu, H. Wang, M. N. Khalil, Q. Hua, X. Qi, *ChemCatChem* **2025**, *17*, e202500298.
- [4] Q. Wang, X. Du, X. Zhang, *Int. J. Hydrogen Energy* **2023**, *48*, 24342-24355.
- [5] M. Kajbafvala, K. Rahimi, B. Eshqi, O. Moradlou, N. Sarikhani, A. Z. Moshfegh, *ACS Appl. Nano Mater.* **2023**, *6*, 21556-21570.
- [6] M. Zhong, W. Li, C. Wang, X. Lu, *Appl. Surf. Sci.* **2022**, *575*, 151708.
- [7] A. Fathollahi, T. Shahrabi, A. Seif, F. Du, J. Li, G. B. Darband, *J. Mater. Chem. A* **2025**, *13*, 18851-18869.
- [8] H. Li, X. Gao, S. Zheng, J. Li, Z. Wang, Z. Shi, J. Bai, X. Wang, *J. Alloys Compd.* **2025**, *1020*, 179554.